

A Wavelet-Based Restricted Earth-fault Power Transformer Differential Protection

M. N. O. Aires, R. P. Medeiros, F. B. Costa, K. M. Silva, J. J. Chavez, M. Popov

Abstract—This paper proposes a restricted earth fault protection based on the wavelet transform (REFW) for detecting ground faults close to the transformer neutral point (turn-to-ground faults) and supporting the conventional phase differential protection, which presents limitations in this kind of faults. The proposed REFW protection uses only high-frequency components instead of phasor estimation, speeding up the detection of turn-to-ground faults. A performance comparison between the proposed wavelet-based restricted earth-fault differential protection and the respective conventional restricted earth-fault (REF) unit was accomplished considering simulated turn-to-ground faults, involving a few winding turns. The proposed method is more efficient and faster than the conventional one, reaching a success rate of 100%.

Index Terms—Power transformer protection, restricted earth fault protection, turn-to-ground faults, wavelet transform.

I. INTRODUCTION

Power transformers are essential components of electric power systems. Due to its importance and cost, its protection must be fast and accurate [1]. Power transformer protection schemes are designed to detect internal faults promptly and present security (i.e., false trip) during external events, such as transformer energization, current transformer (CT) saturation, and over-excitation [2].

Among the power transformer protection schemes, the current percentage differential protection compares the currents that flow through the protected transformer terminals, being the most applied for power transformers rated above 10 MVA [2]. However, some operation conditions, such as transformer energizations and CT saturation, can cause false differential currents, leading to relay misoperation. According to [3], differential relays are prone to incorrectly operate during no-load energization because the inrush currents may be confused with the internal fault currents.

Aiming to improve the performance of the conventional percentage differential relays, harmonic restraint and harmonic blocking logics have been added to the conventional phase differential element [4], [5]. Although it detects most of

internal faults, phase conventional differential units usually present low sensitivity for ground faults close to the transformer neutral point (turn-to-ground faults). However, since the neutral current is high for these cases, a restricted earth-fault (REF) protection is able to successfully detect ground faults close to the neutral point [6]. Indeed, the REF protection is more sensitive in detecting turn-to-ground faults close to the transformer neutral point when compared with another differential protection units [7]. Nevertheless, the REF unit may fail in detecting turn-to-ground faults during inrush conditions because the high harmonic content of the differential current may block the relay tripping [8]. In [9], some traditional REF functions versions are described to discriminate between internal and external events. However, these conventional methods usually present operating delays due to the slow convergence of the phasors when a fault takes place.

Recently, new methods based on artificial intelligence and signal processing techniques have been developed to improve the efficiency of traditional transformer differential protection schemes. Among these algorithms, the wavelet transform has been widely used for this purpose [10]–[13]. For instance, the conventional phase (87T) and the negative sequence (87Q) differential units were recreated by using the real-time boundary stationary wavelet transform (RT-BSWT) in [11]–[13]. Some blocking functions for external event detection, such as sympathetic inrush and external faults, were also proposed in [11]–[13]. Unlike conventional methods that use low-frequency harmonic information, the reported method used high-frequency components of CT secondary currents to be faster and more efficient than the conventional one. However, even though wavelet-based phase (87TW) and negative sequence (87QW) units, the method proposed in [11]–[13] did not consider a function designed to detect challenging turn-to-ground faults close to the transformer neutral point.

This paper proposes the recreation of the traditional REF unit in the wavelet domain, named here as REFW unit, for detecting turn-to-ground faults close to the transformer neutral point, even during transformer energization. The proposed REFW protection uses only high-frequency components induced by faults instead of phasor estimation as conventional REF unit does, speeding up the protection of turn-to-ground faults and being sensitive to this kind of faults during transformer energization. Therefore, the proposed REFW protection can support better differential protection functions. A performance comparison between the proposed wavelet-based REF function and the conventional one was

This work was supported in part by CAPES (Coordenação de Aperfeiçoamento de Pessoal de Nível Superior) and in part by CNPq (Conselho Nacional de Desenvolvimento Científico e Tecnológico).

M. N. O. Aires and F. B. Costa are with the Federal University of Rio Grande do Norte, Natal - RN, Brazil (e-mail: matheus2726@gmail.com; flaviocosta@ect.ufrn.br).

R. P. Medeiros is with the Federal Rural University of the Semi-Arid, Caracás - RN, Brazil (e-mail: rodrigo.prado@ufersa.edu.br).

K. M. Silva is with the University of Brasília, Brasília - DF, Brazil (e-mail: klebermelo@umb.br).

J. J. Chavez and M. Popov are with the Delft University of Technology, Delft, Netherlands (e-mail: m.popov@tudelft.nl; j.j.chavez@muro.tudelft.nl).

accomplished by taking into account turn-to-ground faults on the wye winding, and transformer energizations with turn-to-ground faults in the presence and in the absence of residual flux. The proposed REFW unit ensured a global success rate of 100%. Furthermore, the results revealed that this unit is faster and more efficient than the conventional one.

II. THE PROPOSED WAVELET-BASED REF DIFFERENTIAL PROTECTION

Fig. 1 depicts the flowchart of the proposed wavelet-based REF power transformer differential protection and it is addressed in the remainder of this section.

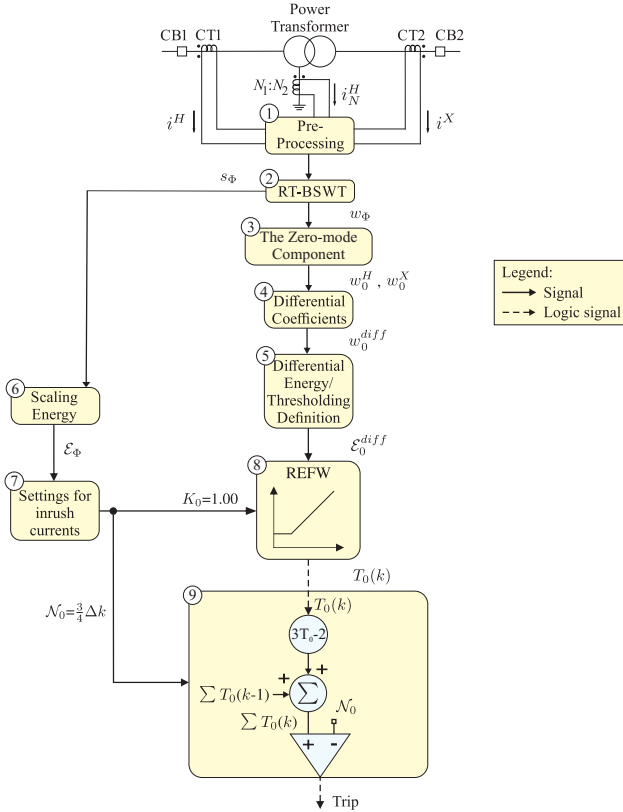


Figure 1. The proposed Clarke-wavelet-based differential protection.

A. Basic Pre-processing (Block 1)

The time-discrete currents $i^H = \{i_A^H, i_B^H, i_C^H\}$, i_N^H , and $i^X = \{i_A^X, i_B^X, i_C^X\}$ are obtained from CT secondary currents considering anti-aliasing filters and A-D converters, where the sub-indices H , X , and N refer to the primary transformer winding, secondary transformer winding, and the neutral point, respectively, whereas A , B , and C refer to phase quantities.

B. RT-BSWT (Block 2)

The RT-BSWT scaling and wavelet coefficients of a current i_Φ are respectively given by [14]:

$$s_\Phi(l, k) = \frac{1}{\sqrt{2}} \sum_{n=0}^{L-1} h_\varphi(n) \overset{\circ}{i}_\Phi(k - L + n + 1 + l), \quad (1)$$

$$w_\Phi(l, k) = \frac{1}{\sqrt{2}} \sum_{n=0}^{L-1} h_\psi(n) \overset{\circ}{i}_\Phi(k - L + n + 1 + l), \quad (2)$$

where $k \geq \Delta k - 1$ is associated to the current sampling time k/f_s ; $0 \leq l < L$ is the border distortion index; h_φ and h_ψ are low-pass scaling and high-pass wavelet filters, respectively; L is the filter length; $\Delta k \geq L$ is the sliding window length; $\overset{\circ}{i}_\Phi(k + m) = \overset{\circ}{i}_\Phi(k - \Delta k + m)$ with $m \in \mathbb{N}^*$, which is a periodized current in Δk samples; $s_\Phi = \{s_A^H, s_B^H, s_C^H, s_A^X, s_B^X, s_C^X\}$ and $w_\Phi = \{w_A^H, w_B^H, w_C^H, w_A^X, w_B^X, w_C^X\}$ are related to $i_\Phi = \{i_A^H, i_B^H, i_C^H, i_N^H, i_A^X, i_B^X, i_C^X\}$.

C. The Zero-mode Components (Block 3)

The zero-mode (0-mode) wavelet coefficients related to the primary and secondary transformer winding currents are respectively given by:

$$w_0^H(k) = \frac{w_A^H(k) + w_B^H(k) + w_C^H(k)}{\sqrt{3}}, \quad (3)$$

and

$$w_0^X(k) = \frac{w_A^X(k) + w_B^X(k) + w_C^X(k)}{\sqrt{3}}. \quad (4)$$

D. Differential Wavelet Coefficients (Block 4)

Based on a classical REF unit, as addressed in [15], this paper proposes the differential 0-mode wavelet coefficients ($w_0^{diff} = \{w_0^{op}, w_0^{res}\}$) instead of 0-mode differential currents as follows:

$$w_0^{op}(0, k) = \frac{1}{2}(\sqrt{3}w_0^H(0, k) + w_N^H(0, k)), \quad (5)$$

$$w_0^{op}(l \neq 0, k) = \sqrt{3}w_0^H(l, k) + w_N^H(l, k), \quad (6)$$

$$w_0^{res}(l, k) = \sqrt{3}w_0^H(l, k), \quad (7)$$

where

$$\sqrt{3}w_0^H(l, k) = w_A^H(l, k) + w_B^H(l, k) + w_C^H(l, k), \quad (8)$$

and $0 \leq l < L$. The superscripts *op* and *res* refer to the operating and restraining variables, respectively.

E. Differential Energy and Threshold Definition (Block 5)

Based on [14], this paper proposes the differential 0-mode wavelet coefficient energies as follows:

$$\mathcal{E}_0^{diff}(k) = \sum_{l=1}^{L-1} [w_0^{diff}(l, k)]^2 + \sum_{n=k-\Delta k+L}^k [w_0^{diff}(0, n)]^2, \quad (9)$$

where $\mathcal{E}_0^{diff} = \{\mathcal{E}_0^{op}, \mathcal{E}_0^{res}\}$.

The threshold related to the energy \mathcal{E}_0^{diff} is statistically defined as follows:

$$E_0^{diff} = \frac{N}{k_2 - k_1 + 1} \sum_{n=k_1}^{k_2} \mathcal{E}_0^{diff}(n), \quad (10)$$

where $[k_1/f_s, k_2/f_s]$ is a previous steady-state time range and $N = 5$. These thresholds are essential for detecting events after the steady-state, such as internal faults, external faults, and transformer energizations.

F. Scaling Coefficient Energy (Block 6)

The scaling coefficient energy is mainly influenced by the smallest frequency components of the currents, which is ideal for identifying null-currents before transformer energization.

Based on [14], the scaling coefficient energies are given by:

$$\mathcal{E}_\Phi(k) = \sum_{l=1}^{L-1} [s_\Phi(l, k)]^2 + \sum_{n=k-\Delta k+L}^k [s_\Phi(0, n)]^2, \quad (11)$$

where $\mathcal{E}_\Phi = \{\mathcal{E}_{sA}^H, \mathcal{E}_{sB}^H, \mathcal{E}_{sC}^H, \mathcal{E}_{sA}^X, \mathcal{E}_{sB}^X, \mathcal{E}_{sC}^X\}$ is the scaling coefficient energy of $i_\Phi = \{i_A^H, i_B^H, i_C^H, i_A^X, i_B^X, i_C^X\}$.

G. Settings for Inrush Currents (Block 7)

The proposed method identifies if the transformer is opened when the currents are lower than the pickup currents, which is accomplished in the wavelet domain as follows:

$$\mathcal{E}_\Phi(k) < E_\Phi, \quad (12)$$

where E_Φ are thresholds related to \mathcal{E}_Φ .

When (12) is true, the trip delay of the REFW unit is set to $\mathcal{N}_0 = \frac{3}{4}\Delta k$. Then, the unit REFW will recognize if the next event results from an inrush current with or without a permanent internal fault.

H. Differential Protection Units (Block 8)

The proposed REFW unit detects an internal fault if:

$$\begin{cases} \mathcal{E}_0^{op}(k) > K_0 \mathcal{E}_0^{res}(k) \\ \mathcal{E}_0^{op}(k) > E_0^{op} \end{cases}. \quad (13)$$

where, the characteristic slope is $K_0 = 1.05$.

The inception time of the internal fault (k_{IF}/f_s) is identified when (13) and

$$\begin{cases} \mathcal{E}_0^{op}(k-1) < E_0^{op} \\ \mathcal{E}_0^{res}(k-1) < E_0^{res} \\ \mathcal{E}_0^{op}(k) > E_0^{op} \\ \mathcal{E}_0^{res}(k) > E_0^{res} \end{cases} \quad (14)$$

are true, where $k_{IF}/f_s = k/f_s$. When (13) is true, the 0-mode energy \mathcal{E}_0^{diff} is in the operation region and the trip command of the REFW unit is high ($T_0(k) = 1$), otherwise \mathcal{E}_0^{diff} is in the restraining region and $T_0(k) = 0$.

I. Trip Management (Block 9)

When the 0-mode energy point is in the restraining region, then $T_0(k) = 0$. Therefore, the operator $3T_0 - 2 = -2$, which produces a decrease by 2 in the trip counter $\Sigma T_0(k)$, where $\Sigma T_0(k) \geq 0$. Conversely, when the 0-mode energy point is in the operating region, then $T_0(k) = 1$. As a consequence, $3T_0 - 2 = 1$, which produces an increase in the trip counter $\Sigma T_0(k)$. Thereafter, $\Sigma T_0(k)$ is compared to the related trip delay \mathcal{N}_0 , where the relay trips when $\Sigma T_0(k) > \mathcal{N}_0$ (Fig. 1). The default trip delay \mathcal{N}_0 is zero. However, it can be changed according to Sections II-G.

III. PERFORMANCE ASSESSMENT

The performance of the proposed protection scheme is assessed by performing several fault conditions in the power system shown in Fig 2, which was modeled in the ATP. The power system is represented by two equivalent sources (S1 and S2), two 100 MVA, 230/69 kV power transformers configured at YNd1 (T1 and T2). The 230 kV and 69 kV CTs are connected at 500/5 A and 1200/5 A taps, respectively. More details about the modeled power system can be found in the Appendix.

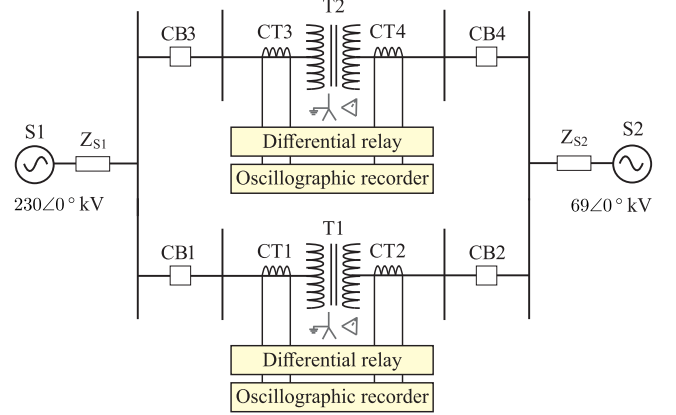


Figure 2. Single line diagram of the electrical system.

Since the proposed wavelet-based differential protection needs to detect high-frequency transients induced by internal faults, it uses a sampling frequency of 15360 Hz, which is suitable for this purpose. Besides, modern relays can use a similar sampling frequency in a practical application. The proposed REFW method uses the Daubechies mother wavelet with four coefficients (db(4)).

The performance of the proposed method is compared to the traditional phasor-based REF differential function shown in [15]. Also, based on [16], the REF was supervised by an harmonic blocking function. The full-cycle Fourier algorithm estimates the complex phasors. This method uses a conventional sampling frequency of $f_s = 960$ Hz, which is appropriated for estimating fundamental and low-order harmonic components. A higher sampling frequency, such as 15360 Hz, would not speed up the relay operating time, and the phasor estimation could be susceptible to high-frequency components.

The performance of the REF-based units was assessed with a database with representative events, as follows:

- 1) Database 1 (turn-to-ground faults): turn-to-ground faults on the phase A wye winding. The percentage of the turns in the fault is equal to $e = \{1, 2, 3, \dots, 98\}\%$ (98 records).
- 2) Database 2 (transformer energizations with turn-to-ground faults in the absence of residual flux): switching performed by the high voltage side (230 kV) of the transformer, with its secondary terminal opened (CB2 opened), changing the high voltage circuit-breaker closing time at the angle θ_s electrical

degrees for each case listed on the database 1 (98 records).

- 3) **Database 3 (transformer energization with turn-to-ground faults in the presence of residual flux):** the same cases of the database 2, but considering the existence of residual flux ($\varphi_{res} = 50$ Wb) in the power transformer core.

Databases 1, 2 and 3 consider a typical signal-to-noise ratio (SNR) of 60 dB. The REFW unit is an auxiliary function to the differential protection to detect only turn-to-ground faults. Therefore, other events such as external faults and overexcitation were not in the scope of presented research in this paper because the differential protection blocks the REF-type functions during external events.

Table I describes the settings used for the conventional protection scheme, whereas Table II presents the performance of the proposed and conventional REF units, whose explanations are addressed in the remainder of this section.

Table I

THE CONVENTIONAL PROTECTION SCHEME PARAMETERIZATION [15]

REF		Harmonic Blocking	
$SLP3$	I_{puR}	K_{2b}	K_{5b}
1.05	0.2	0.15	0.15

A. Turn-to-Ground Faults (Database 1)

According to Table II, the proposed REFW unit presented a success rate of **100%** for all turn-to-ground faults (database 1). Moreover, the average operating time was **65.1 μ s**, which is a fast power transformer restricted earth-fault protection. Although the conventional REF unit also shows a success rate of **100%**, its average operating time was **14.1 ms**. Therefore, the REFW unit is **the fastest** because it uses only fault-induced high-frequency transients, which can be detected in few microseconds with the wavelet transform. Conversely, the conventional REF unit operates with delays because there is a delay in the convergence of the phasor estimation algorithm from the fault inception time. Also, the high-level of harmonic content of the differential current leads to the blocking of the relay operation during the transient period of the fault.

Figs. 3 and 4 depict the performance of the proposed REFW unit during a critical turn-to-ground fault which involve 5% of the turns of the phase A wye winding. The energies \mathcal{E}_0^{op} and \mathcal{E}_0^{res} presented a hard increase soon after the fault inception time (Fig. 3), thereby the internal fault is detected successfully and a trip command is provided when $\mathcal{E}_0^{op} \gg \mathcal{E}_0^{res}$, which occurs around **65.1 μ s** (Fig. 4).

B. Transformer Energizations with Turn-to-Ground Faults in the Absence of Residual Flux (Database 2)

According to Table II, the proposed REFW unit protected the entire wye winding for all turn-to-ground faults during transformer energizations (**100%** of success rate). Due to presence of inrush currents, the trip delay of the REFW unit was changed for $\mathcal{N}_0 = \frac{3}{4} \Delta k$ and an average operating

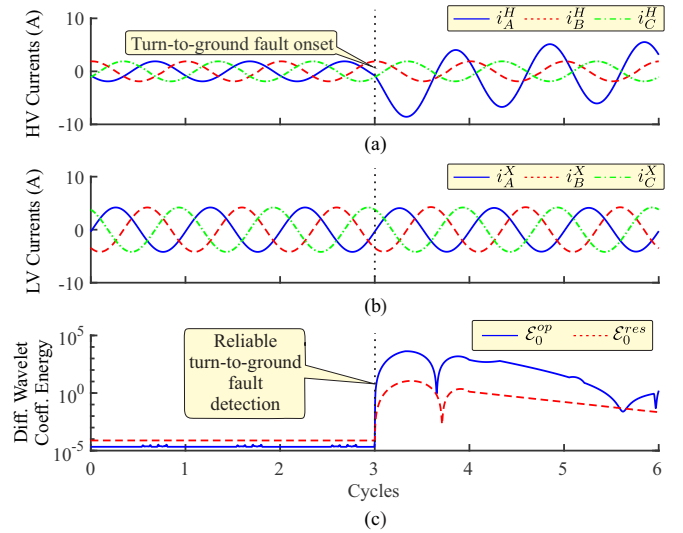


Figure 3. Turn-to-ground fault: (a) i_A^H, i_B^H, i_C^H ; (b) i_A^X, i_B^X, i_C^X ; (c) Zero-mode differential energies \mathcal{E}_0^{op} and \mathcal{E}_0^{res} .

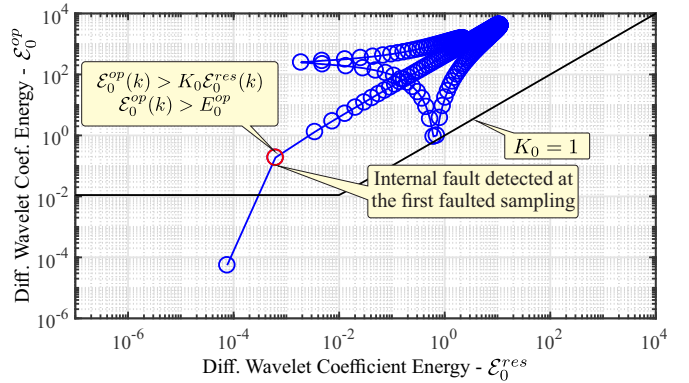


Figure 4. Zero-mode energy operating points during one cycle of a turn-to-ground fault.

time of about **14.9 ms** was achieved. The conventional method presented an average operating time of about **17.3 ms**, which was higher than the proposed REFW unit. Besides, the conventional REF protection ensured a success rate of **90.82%**, failing to detect faults in a small portion of winding (from 1% to 9% of the turns, totalizing 9 events). The high harmonic content present in healthy phases during the **1-9% turn-to-ground** faulted transformer energizations blocked the trip of the conventional relay.

Figs. 5 and 6 depict, respectively, the performance of the proposed REFW unit for a turn-to-ground fault involving 5% of the turns to the neutral in phase A of the wye winding occurring at the same time of a transformer energization, and the trajectory of the zero-mode energy operating points during the first cycle after the energization initiation. According to Fig. 5(c), the energies \mathcal{E}_0^{op} and \mathcal{E}_0^{res} presented a hard increase from the beginning of the events and the internal fault in phase A was successfully detected. Then, a trip command was issued when $\mathcal{E}_0^{op} \gg \mathcal{E}_0^{res}$, with an average delay of about **13.1 ms**. Conversely, the trip of the conventional REF was blocked by the harmonic blocking unit due to the high harmonic content in the inrush current in phases B and C.

Table II
PERFORMANCE ASSESSMENT OF THE METHOD FOR THE SIMULATED DATABASES

Event	Total cases	Proposed method				Conventional method			
		Trips	No trips	Success rate (%)	Average oper. time	Trips	No trips	Success rate (%)	Average oper. time
Turn-to-ground faults	98	98	0	100%	65.1 μ s	98	0	100%	14.1 ms
Faulted transformer energizations	98	98	0	100%	14.9 ms	89	9	90.82%	17.3 ms
Faulted transformer energizations with initial flux	98	98	0	100%	15.0 ms	91	7	92.86%	14.7 ms

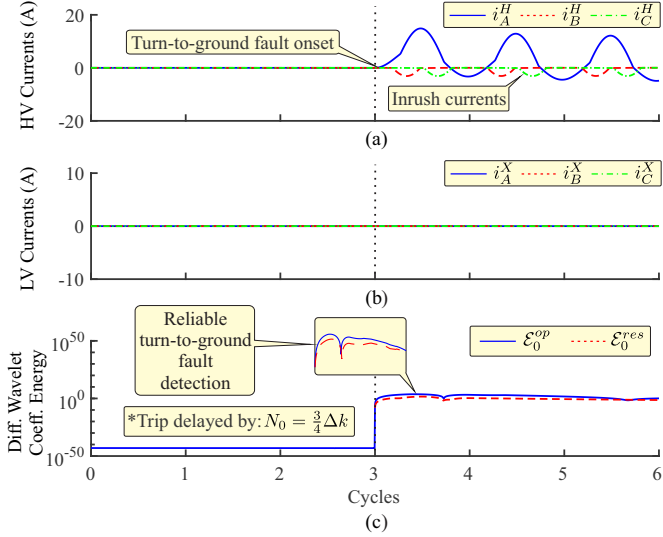


Figure 5. Transformer energization with turn-to-ground fault: (a) i_A^H, i_B^H, i_C^H ; (b) i_A^X, i_B^X, i_C^X ; (c) Zero-mode differential energies \mathcal{E}_0^{op} and \mathcal{E}_0^{res} .

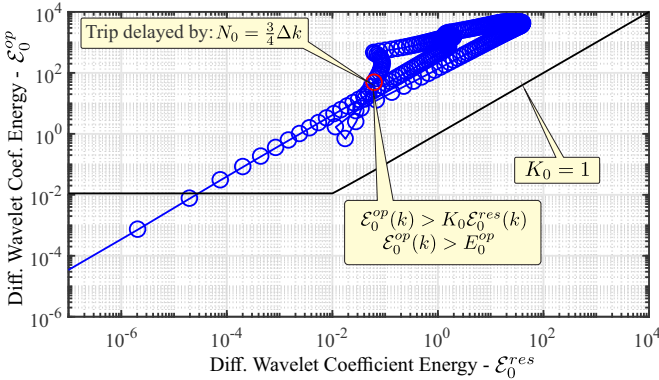


Figure 6. Zero-mode energy operating points during one cycle of the transformer energization with turn-to-ground fault.

An example of the proposed method performance for transformer energizations in the absence of faults is shown in Fig. 7, which depicts the CT currents and the zero-mode differential energies when T1 is energized by the high voltage side (230 kV) with its secondary terminal opened (CB2 opened). The high voltage circuit breaker was closed when the voltage angle of phase A was equal to 0°. According to Fig 7(c), the energies \mathcal{E}_0^{op} and \mathcal{E}_0^{res} hard increased during the beginning of the event. However, the REFW unit operated

with a delay equal to $N_0 = \frac{3}{4} \Delta k$ in the transformer energization detection mode, and no internal fault was wrongly detected.

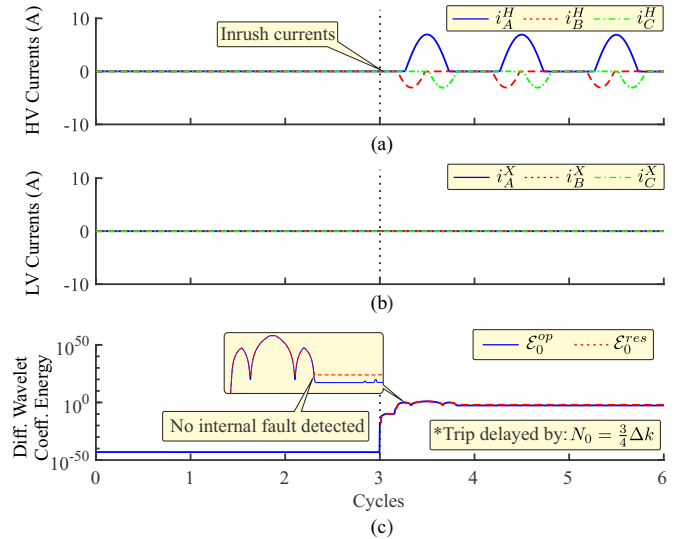


Figure 7. Transformer energization: (a) i_A^H, i_B^H, i_C^H ; (b) i_A^X, i_B^X, i_C^X ; (c) Zero-mode differential energies \mathcal{E}_0^{op} and \mathcal{E}_0^{res} .

The trajectory of the zero-mode energy operating points during the first cycle after the event initiation for the energization case presented in Fig. 7 is presented in Fig 8. According to Fig 8, the proposed method identifies the inrush currents and set the trip delay ($N_0 = \frac{3}{4} \Delta k$) such that no fault is detected. The trip delay is necessary to ensure no trip command is issued during the energization maneuver.

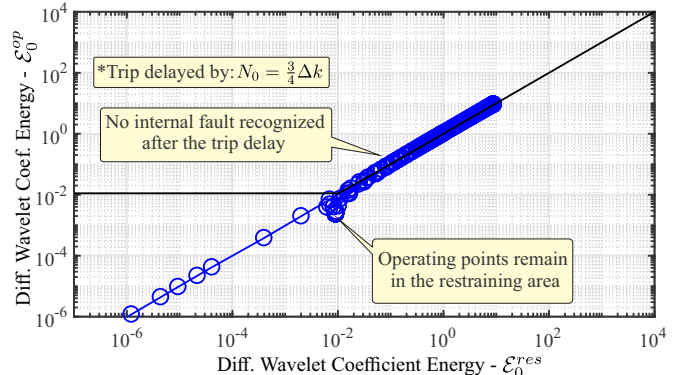


Figure 8. Zero-mode energy operating points during one cycle of the transformer energization.

C. Transformer Energization with Turn-to-Ground Faults considering Residual Flux (Database 3)

Power transformers usually present a certain level of residual magnetism in practical situations because of their constant magnetization and desmagnetization, which should be taken into account in simulation models. According to Table II, the proposed method detected all turn-to-ground faults of database 3, ensuring a success rate of 100% with an average operating time of 15 ms. Therefore, the proposed method was reliable and scarcely affected by the residual flux variation in the power transformer.

Regarding the conventional REF, this unit presented a slight improvement in its performance with a success rate of 92.86% and an average operating time of about 14.7 ms. According to [17], the fundamental component of the inrush current is increased during transformer energizations with residual flux, whereas its second harmonic content decreases depending on the quantity of the residual magnetism, which could reduce the security of the conventional differential protection relay. In these conditions, if a fault occurs during a transformer energization, the protection is expected to operate [17].

IV. CASE STUDY: SYMPATHETIC INRUSH

A sympathetic inrush condition occurs when a power transformer is switched on in a substation which has other already previously energized transformers [18]. In this case, inrush currents are generated in both switched and operating transformers. The challenging is because the inrush current presents other harmonic components, such as the second one, and a dc component, which can saturate the transformer, causing undesired distorted differential currents. Therefore, this event can lead to a failure of some differential function such as the REF one. This problem can be overcome with blocking functions. For instance, the second harmonic has been used by the conventional differential protection to block the negative-sequence and REF elements in these situations [16]. In the same fashion, blocking elements can be used to block the operation of the proposed REFW protection function.

A block function to the proposed REFW is out of scope of this paper. However, an existing external event detection method for power transformer based on the wavelet transform, such as that proposed by [12], could be used. For instance, the external event detection method proposed in [12] detects a sympathetic inrush when the restraining wavelet coefficient energy presents a high increase whereas the operating wavelet coefficient energy does not increase at the same rate. These energy components can be computed from α -mode components (\mathcal{E}_α^{op} , \mathcal{E}_α^{res}). Therefore, when $\mathcal{E}_\alpha^{res} \gg \mathcal{E}_\alpha^{op}$ at the beginning of an event, then the proposed REFW could be blocked. To show this possibility, the performance of the proposed method in association with the blocking function proposed in [12] was assessed considering an example of sympathetic inrush condition.

Fig. 9 depicts a sympathetic inrush condition simulated in the power system shown in Fig. 2 considering the power transformer T1 previously energized (CB1 and CB2 closed) and with the switching performed by the high voltage side

of T2, with its secondary terminal opened (CB4 opened). At the beginning of the event, distortions in the currents generated high-frequency components, increasing both the zero-mode differential energies (Fig. 9(c)). Therefore, this situation would lead to a false trip by the REFW. Nevertheless, as the conventional REF function, the REFW function was designed to be sensitive to grounded internal faults, needing a block function in this case as aforementioned. According to Fig. 9(d), an external event would be detected ($\mathcal{E}_\alpha^{res} \gg \mathcal{E}_\alpha^{op}$) and the REFW function would be blocked.

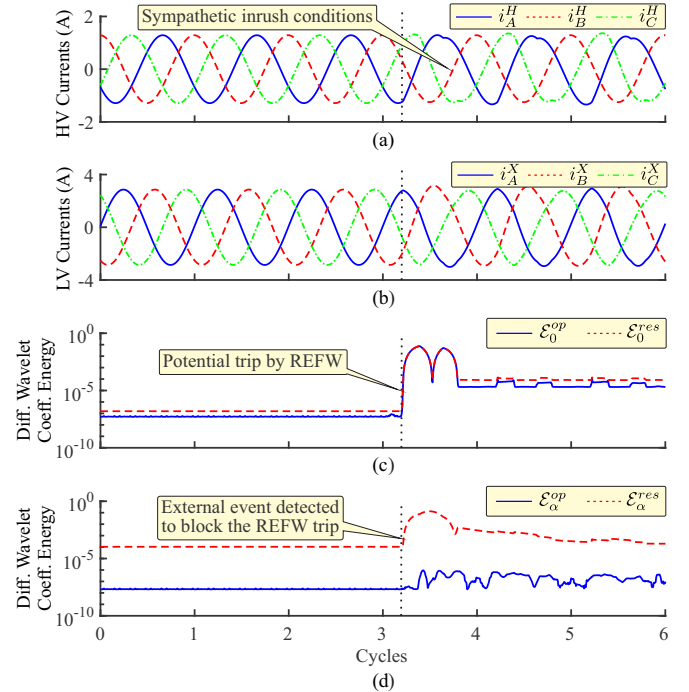


Figure 9. Sympathetic inrush condition: (a) i_A^H , i_B^H , i_C^H ; (b) i_A^X , i_B^X , i_C^X ; (c) Zero-mode differential energy components \mathcal{E}_0^{op} and \mathcal{E}_0^{res} . (d) Alpha-mode differential energy components \mathcal{E}_α^{op} and \mathcal{E}_α^{res} .

V. CONCLUSION

This paper presents a new time-domain restricted earth-fault power transformer differential protection based on the wavelet transform. Based on the obtained results, the proposed REFW method can be successfully used for turn-to-ground faults and transformer energization with turn-to-ground faults, even when there is residual flux, because it presented 100% of success rate. In contrast, the phasor-based conventional protection failed in some transformer energizations with turn-to-ground faults and also in cases with residual flux. Besides, the average relay operating time of the REFW was faster than that of the conventional method, which presented an operation time delay of almost a cycle due to phasor filtering process. Moreover, the proposed method shows good behavior in detecting inrush currents, without false trips when this type of event occurs. The trip delay applied in this case ensured that the method recognizes if some permanent internal fault arises.

As REFW uses the high-frequency content of the currents, it is not affected by low-frequency harmonics, whose variations can affect the performance of conventional methods, especially

in inrush conditions, as reported in this paper. Finally, considering the existing trends in the development of signal processing technology, REFW could be a promising solution to enhance transformer protection.

VI. APPENDIX

A. Thevenin Equivalents

Table III presents the source and impedance data of the Thevenin equivalents.

Table III
THEVENIN EQUIVALENTS DATA.

Source	Voltage	SIR	Z_0 (Ω)	Z_1 (Ω)
S1	$230\angle 0^\circ$ kV	0.1	$2.86 + j23.13$	$2.51 + j24.78$
S2	$69\angle -45^\circ$ kV	0.1	$5.52 + j8.61$	$4.02 + j6.26$

B. Power Transformer Model

Power transformer model is provided by [11], having rated power of 100 MVA, voltage ratio of $V_p:V_s = 230:69$ kV, and YNd1 configuration. The impedances related to the primary and secondary windings of the power transformers T2 and T3 are $R_p + jX_p = 2.04 + j12.54 \Omega$ and $R_s + jX_s = 1.44 + j38.04 \Omega$, respectively. The current versus flux (i , φ) magnetizing characteristic was modeled by HYSTERESIS HEVIA ATP routine as presented in Table IV.

Table IV
NONLINEAR CHARACTERISTICS OF THE MAGNETIZING BRANCH OF T2, T3, CT1, AND CT2.

T2 and T3				CT1 (800-5 A)		CT2 (1200-5 A)	
i (A)	φ (Wb)	i (A)	φ (Wb)	i (A)	φ (Wb)	i (A)	φ (Wb)
-15.594	0.478	-591.538	523.044	0.003	0.004	0.001	0.004
-8.953	1.211	-585.312	547.951	0.005	0.011	0.003	0.011
-6.446	2.540	-579.085	572.858	0.008	0.019	0.004	0.019
-2.540	6.446	-572.858	579.085	0.013	0.041	0.006	0.045
-1.211	8.953	-547.951	585.312	0.020	0.075	0.010	0.113
-0.478	15.594	-523.044	591.538	0.032	0.188	0.038	0.375
-0.144	20.396	-498.137	597.765	0.053	0.375	0.081	0.750
0.000	35.461	0.000	603.992	0.114	0.750	0.203	1.500
0.144	498.137	15.071	1.125	28.762	1.876		

C. Current Transformer Model

The leakage inductances and resistances related to the losses on the primary and secondary CT windings are taken from [19]. Data concerning non-linear modeling of the CT (saturation curve) are taken from [20]. Fig. 10 depicts the equivalent circuit model for the CTs.

ATP's SATURATION support routine is used to convert the original $v-i$ characteristic curves of the CTs provided by [20] into an equivalent $\varphi-i$ data set. Then, the magnetizing branch is modeled in ATP using the card type 98. The current versus flux (i , φ) magnetizing characteristics of the CTs are described in Table IV.

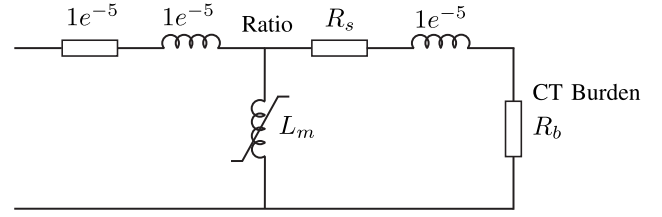


Figure 10. The CT circuit model used in this work.

REFERENCES

- [1] M. Tripathy, R. P. Maheshwari, and H. K. Verma, "Power transformer differential protection based on optimal probabilistic neural network," *IEEE Transactions on Power Delivery*, vol. 25, no. 1, pp. 102–112, 2010.
- [2] J. L. Blackburn and T. J. Domin, *Protective Relaying: Principles and Applications, Third Edition*. Taylor & Francis, 2006.
- [3] E. A. Klingshirn, H. R. Moore, and E. C. Wentz, "Detection of faults in power transformers," *Electrical Engineering*, vol. 76, no. 4, pp. 295–295, 1957.
- [4] K. Behrendt, N. Fischer, and C. Labuschagne, "Considerations for using harmonic blocking and harmonic restraint techniques on transformer differential relays," *Journal of Reliable Power*, vol. 2, no. 3, pp. 36–52, 2011.
- [5] A. Guzman, N. Fischer, and C. Labuschagne, "Improvements in transformer protection and control," in *62nd Annual Conference for Protective Relay Engineers*, March 2009, pp. 563–579.
- [6] H. Ferrer and E. Schweitzer, *Modern Solutions for Protection, Control, and Monitoring of Electric Power Systems*. Schweitzer Engineering Laboratories, Incorporated, 2010.
- [7] T. Ghanbari, H. Samet, and J. Ghafourifard, "New approach to improve sensitivity of differential and restricted earth fault protections for industrial transformers," *IET Generation, Transmission Distribution*, vol. 10, no. 6, pp. 1486–1494, 2016.
- [8] M. Davarpanah, M. Sanaye-Pasand, and R. Iravani, "Performance enhancement of the transformer restricted earth fault relay," *IEEE Transactions on Power Delivery*, vol. 28, no. 1, pp. 467–474, 2013.
- [9] "IEEE guide for protecting power transformers," *IEEE Std C37.91-2008 (Revision of IEEE Std C37.91-2000)*, pp. 1–139, May 2008.
- [10] S. A. Saleh, B. Scaplen, and M. A. Rahman, "A new implementation method of wavelet-packet-transform differential protection for power transformers," *IEEE Trans. Ind. Applications*, vol. 47, no. 2, pp. 1003–1012, 2011.
- [11] R. P. Medeiros, F. B. Costa, and K. M. Silva, "Power transformer differential protection using the boundary discrete wavelet transform," *IEEE Trans. Power Del.*, vol. 31, no. 5, pp. 2083–2095, Oct 2016.
- [12] R. P. Medeiros and F. B. Costa, "A wavelet-based transformer differential protection with differential current transformer saturation and cross-country fault detection," *IEEE Trans. Power Del.*, vol. 33, no. 2, pp. 789–799, Apr 2018.
- [13] R. P. Medeiros and F. B. Costa, "A wavelet-based transformer differential protection: Internal fault detection during inrush conditions," *IEEE Trans. Power Del.*, vol. 33, no. 6, pp. 2965–2977, Dec 2018.
- [14] F. B. Costa, "Fault-induced transient detection based on real-time analysis of the wavelet coefficient energy," *IEEE Trans. Power Del.*, vol. 29, no. 1, pp. 140–153, Feb 2014.
- [15] B. N. Taj, A. Mahmoudi, and S. Kahourzade, "Comparison of low-impedance restricted earth fault protection in power transformer numerical relays," *Australian Journal of Basic and Applied Sciences*, 2011.
- [16] K. Antunes Tavares and K. Melo Silva, "Evaluation of power transformer differential protection using the atp software," *IEEE Latin America Transactions*, vol. 12, no. 2, pp. 161–168, 2014.
- [17] R. Hamilton, "Analysis of transformer inrush current and comparison of harmonic restraint methods in transformer protection," *IEEE Trans. Ind. Applications*, vol. 49, no. 4, pp. 1890–1899, July 2013.
- [18] H. S. Bronzeado, P. B. Brogan, and R. Yacimini, "Harmonic analysis of transient currents during sympathetic interaction," *IEEE Transactions on Power Systems*, vol. 11, no. 4, pp. 2051–2056, Nov 1996.
- [19] IEEE Power System Relaying Committee, "EMTP reference models for transmission line relay testing," 2004.

- [20] IEEE Std C37.110-2007, "IEEE guide for the application of current transformers used for protective relaying purposes - redline," pp. 1-83, April 2008.